

Widespread active detachment faulting and core complex formation near 13°N on the Mid-Atlantic Ridge

Deborah K Smith¹, Johnson R Cann² & Javier Escartín³

*1*Woods Hole Oceanographic Institution, Woods Hole Massachusetts 02543, USA

*2*School of Earth Sciences, University of Leeds, Leeds LS2 9JT, UK

*3*CNRS, Marine Geosciences Group, IPGP Case 89, Paris 75252 Cedex 05, France

Oceanic core complexes are massifs in which lower crustal and upper mantle rocks are exposed at the sea floor¹⁻³. They form at mid-ocean ridges through slip on detachment faults rooted below the spreading axis²⁻⁶. To date, most studies of core complexes have been based on isolated inactive massifs that have spread away from ridge axes. A new survey of the Mid-Atlantic Ridge (MAR) near 13°N reveals a segment in which a number of linked detachment faults extend for 75 km along one flank of the spreading axis. The detachment faults are apparently all currently active and at various stages of development. A field of extinct core complexes extends away from the axis for at least 100 km. The new data document the topographic characteristics of actively-forming core complexes and their evolution from initiation within the axial valley floor to maturity and eventual inactivity. Within the surrounding region there is a strong correlation between detachment fault morphology at the ridge axis and high rates of hydroacoustically-recorded earthquake seismicity. Preliminary examination of seismicity and seafloor morphology farther north along the MAR suggests that active detachment faulting is occurring in many segments and that detachment faulting is more important in the generation of ocean crust at this slow-spreading ridge than previously suspected.

The existence of low-angle faults extending deep below the axes of mid-ocean ridges⁷ has long been inferred from seafloor exposures of deep-seated rocks. Direct evidence for such faults has only recently come from bathymetry^{1,2}, and seafloor sampling and drilling^{4,5,8}. The faults are corrugated parallel to the spreading direction and cap smooth topographic highs, termed oceanic core complexes, where deep-seated rocks such as gabbros and serpentized peridotites are exposed^{4,5,9,10}. Most core complexes have been identified towards the ends of spreading segments where magma supply appears to be low, but in places they extend for tens of kilometers parallel to the axis^{4,5,11-13}. In parts of some segments, extension by low-angle faulting may have accounted for >50% of the total extension by spreading^{3,10,14}. Because almost all core complexes identified to date are far enough from the axis to be inactive, the nature of active detachment faults is controversial. How do they initiate? How do they evolve as they emerge from the ocean floor? How is active detachment faulting accommodated along the length of the spreading axis? Is there a seismic signature to detachment faulting? We answer these questions using a new survey of the MAR near 13°N together with existing multibeam bathymetry and

hydroacoustically-recorded seismicity, and extend our conclusions to other mid-ocean ridge segments in the region.

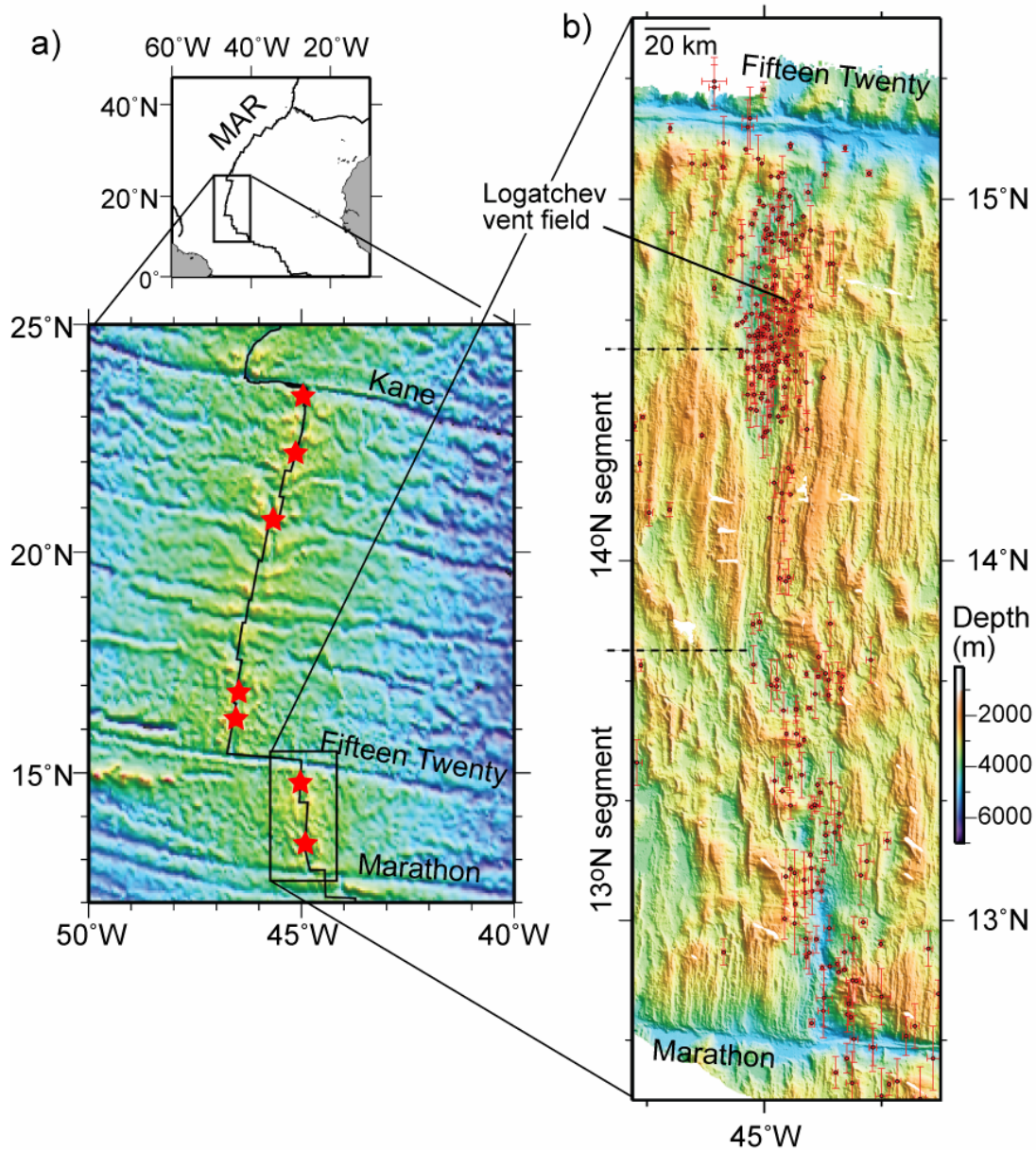


Figure 1. Location map and bathymetry near 13°N on the Mid-Atlantic Ridge (MAR). a) Top: MAR axis. Bottom: satellite altimetry data¹⁵. Red stars: seven sections of the axis showing persistent, high levels of hydroacoustically-recorded seismic activity¹⁶. b) Multibeam bathymetry from Smith and Escartin, Fujiwara et al.¹⁷, and Escartin and Cannat¹¹. The “14°N Segment” has faulted volcanic morphology, while the segments to the north and south have irregular and blocky topography and core complexes. The peridotite-hosted Logatchev hydrothermal vent field¹⁸ is marked. Red dots: locations of 292 hydroacoustically-detected events for the period 1999-2005 with 1 σ error bars¹⁶ $\leq \pm 10$ km.

A bathymetric map of the MAR between the Fifteen-Twenty and the Marathon fracture zones (Fig. 1) shows an alternation in the morphology of the spreading axis. Of the two major segments in this area, that between 14°35'N and 13°50'N (labeled 14°N Segment) has a volcanic signature, with closely-spaced volcanic ridges on both

flanks, tens of kilometers long, and cut by steep inward-facing faults. The segment to the south between 13°50'N and 12°40'N (13°N Segment) has more chaotic topography. The west flank, in particular, is very distinctive with widely-spaced, narrow ridges, typically <20 km long, that have steep slopes dipping away from the spreading axis, and are separated by areas of smoother seafloor. As shown below, a large part of this smoother seafloor is corrugated parallel to the spreading direction.

In well-explored oceanic core complexes the existence of a corrugated surface is correlated with detachment faulting and exposures of deep-seated rocks^{1-4,6}. Consequently, corrugations have been used to identify other core complexes in regions with limited data². Corrugations have a wavelength of hundreds of meters and an amplitude of tens of meters^{1,3}, and can be seen on shaded relief maps of multibeam bathymetry data. The origin of the corrugations is still enigmatic. Direct observations have shown that they are not produced by faults parallel to the spreading direction^{14,19}. One possibility is that they originate by continuous casting²⁰ of a ductile footwall by irregularities in a strong and brittle hanging wall.

An inactive, corrugated core complex near 30°N¹ at the MAR (Fig. 2) shows other characteristics common to core complexes. First, a steep (25-30°) slope faces away from the axis at the older edge (scarps at slow- and intermediate-spreading ridges typically face towards the axis²¹). Second, a narrow, linear ridge parallel to the axis caps the outward-facing slope^{1,2} and extends beyond the corrugated surface. Dredge samples from the linear ridge in Fig. 2 show that it is composed of basalt¹ and thus is probably volcanic seafloor created at the axis. Finally, a steep normal fault dips towards the spreading axis truncating the corrugated surface on its younger side.

In the 13°N Segment, corrugated surfaces and outward facing steep slopes dominate the western flank of the spreading center, extending for 75 km along axis and >100 km across axis (Fig. 3a). The feature centered at 13°10'N, 45°00'W (labeled '1' on Fig. 3a) is typical of many of those observed off-axis, and has a similar morphology to that of Fig. 2. The morphology and spatial scale of this and other corrugated surfaces and ridges in the 13°N Segment indicate that the evolution of the western flank involves repeated detachment faulting and core complex formation.

Two core complexes north of complex '1' at 13° 20'N, 44°55'W (labeled '2' on Fig. 3a,b) and 13° 30'N, 44°55'W (labeled '3') have a different morphology from the core complexes that lie off axis. Each extends ~10 km along axis and is close to the spreading axis. The corrugated surfaces are domes that meet ridges to the west, and curve over to the east, dipping at 15° to meet the axial valley floor. Instead of being truncated by later faults, as with the off-axis core complexes, the slope at the east end of each of the domes intersects the median valley floor along a curved line <5 km from the volcanic axis (Fig. 3). These features suggest that the domes are the surfaces of detachment faults actively emerging from the valley floor.

We also identify a larger and apparently compound core complex extending for 30-40 km parallel to the axis (labeled 'C' on Fig. 3a, stretching from 12° 55'N to 13°10'N). This compound core complex includes complex '1' and another similar complex to the south (labeled '4') linked by a third complex located ~5 km to the

east. This third complex terminates in a boundary with the volcanic morphology of the valley floor that is convex towards the east. A corrugated surface is present over a large part of the linking complex.

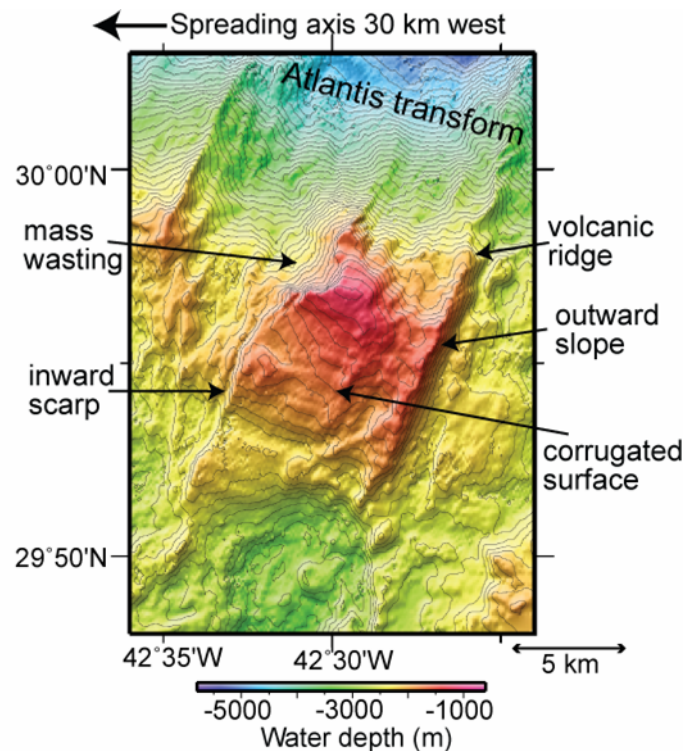


Figure 2. Bathymetry map (100-m contour intervals) of a well-explored, extinct core complex south of the Atlantis fracture zone on the MAR³. The complex has been spread ~30 km east of the axis. Its morphological characteristics include an outward-facing slope with a volcanically constructed ridge capping the core complex on the older (outer) side. A normal (inward-facing) fault scarp cuts the feature on its younger (inner) side. Corrugations running parallel to spreading direction cap the shallow-dipping top. Serpentinized peridotite was recovered by dredging the corrugated surface⁷. Mass wasting of the massif is indicated by the scoop on its northwest corner.

Because many of the core complexes in this segment have straight narrow ridges at their outer sides, we consider linear ridges as possible precursors to the emergence of the detachment faults. Such ridges occur in several places close to the spreading axis (labeled 'R' on Fig. 3a,b), each backed by a deep basin (Fig. 3). The outer slopes of the ridges dip at 15-20° away from the axis and show a hummocky volcanic morphology similar to those of the ridges farther from the spreading axis. Presumably they form by rotation of sections of volcanic seafloor away from the axis. We infer that the ridges mark the breakaway zones of detachment faults.

The strong morphologic evidence for active detachment faulting led us to search for associated seismic activity. Traditionally, seismically active MAR segments have been identified by locating foci of earthquakes of magnitude >4.5 detected by land seismometers, but their locations are poorly constrained, and these earthquakes are few in number. Between 1999-2005 an autonomous hydrophone array in the North

Atlantic²² recorded the hydroacoustic energy from thousands of earthquakes of smaller magnitude (>2.5). Hydroacoustic events are better located than those detected teleseismically^{22,23}, and clearly show the currently active sections of MAR segments¹⁶. Two sections of ridge between the Fifteen-Twenty and Marathon fracture zones (Fig. 1b) show relatively high and persistent seismicity²⁴, and are separated by the seismically quiet 14° N Segment. Core complexes have been identified in the active segment just south of the Fifteen-Twenty fracture zone¹⁷. The other seismically active section, the 13° N Segment, is active along its entire length, with no obvious spatial or temporal clustering of events. Location errors (Fig.1b) are large enough, though, that events cannot be associated with individual detachments, nor with possible seismic sources associated with core complex formation.

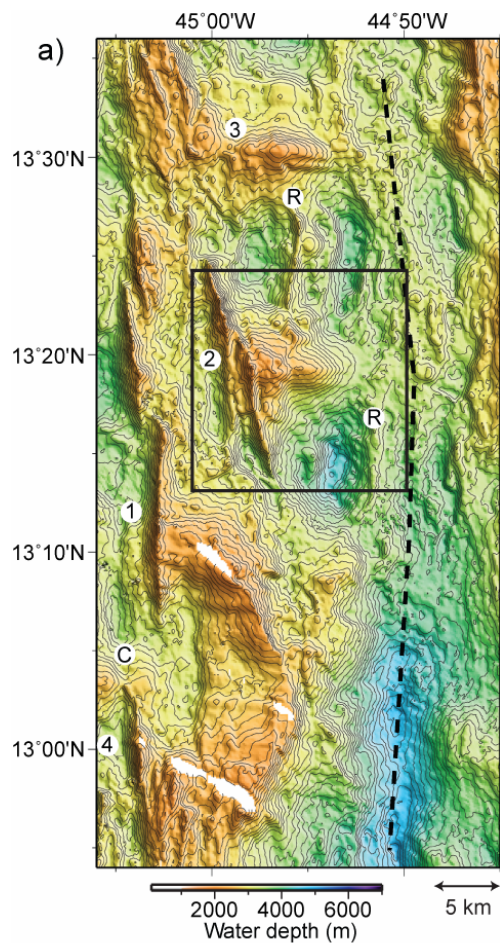
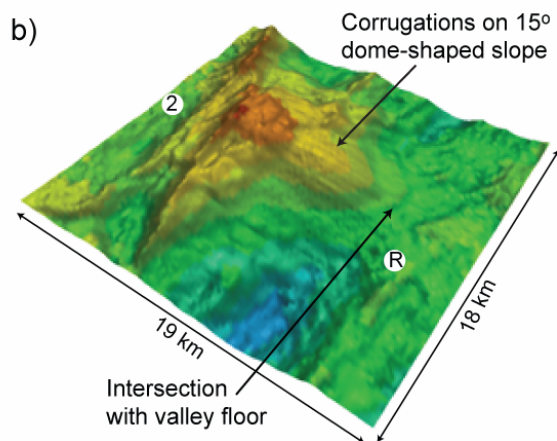


Figure 3. Multibeam bathymetry showing detachment faults and core complexes in the 13°N segment. a) Map contour interval is 100 m. Linked and active core complexes extend 75km along the axis. The dashed line indicates the spreading axis. The box indicates the location of the image in (b). R, topographic ridges, inferred to be breakaways for new detachment surfaces. Numbers, complexes discussed in the text. C, compound core complex composed of complexes '1' and '4' and a third linking complex. b) Three-dimensional perspective view of complex '2' with no vertical exaggeration. The corrugated surface and its intersection with the sea floor are marked.



The seismic evidence supports the morphologic evidence that a 75-km long chain of detachment faults on the western side of the axial valley is active. Some of the detachment faults are mature (complexes '1' and '4' on Fig. 3a), some are in the early stages of development ('2' and '3'), and some are in an incipient stage of evolution, as shown by the narrow ridges close to the spreading axis ('R'). As they evolve and spread away from the axis, the detachments become inactive and new detachments initiate within a few kilometers of the axis.

Because of the number of core complexes at different stages of evolution, we can reconstruct the evolution of a core complex from initiation to maturity to inactivity (Fig. 4). The first stage is the subsidence of a basin within the axial valley floor, coupled with the emergence of a narrow basaltic ridge (Fig. 4a). The basin lies immediately behind the ridge, and probably forms by outward footwall rotation as a new fault initiates. The inner (eastern) side of the basin (and hence the outer side of the ridge) has the volcanic morphology of the axial valley floor, tilted at 15°-25°. As the ridge evolves, the tilt of the outer slope increases to 20°-30°. A fault scarp dipping at 15°-25° emerges on the inner side of the ridge.

The next stage is the emergence of a domal corrugated fault surface that intersects the valley floor along a line convex towards the spreading axis (Fig. 4b). The corrugated surface dips at ~15° where it plunges into the valley floor. The dip of the surface gradually flattens as it emerges due to flexure of the footwall, and by ~5 km from its emergence the crest is nearly horizontal. Below the median valley floor, the detachment fault may continue at a low angle, but the early rotation of the footwall to form the basin suggests that the fault curves and steepens below the seafloor, so that the tip of the fault may lie several kilometers down.

The resulting mature core complex (Fig. 4c) becomes extinct when it is cut off by a normal fault. At that stage the domal surface flattens until it is close to horizontal. In some places, the core complex may extend as a single elongate unit from tens to over a hundred kilometers from the spreading axis, as observed in the Australian-Antarctic Discordance^{9,10} and the Parece Vela Basin¹². In our study area, the small spacing between breakaway faults indicates a short life for any individual complex and regular nucleation of new detachment faults in the median valley.

Because of the apparent correlation of persistent earthquake seismicity and core complex morphology, we examined a larger region of the MAR (24°-15°N) to look for additional sites of active core complex formation. We identified five ridge sections with high levels of hydroacoustically-recorded seismic activity¹⁶ (Fig. 1a). The seismicity is persistent and not triggered by large earthquakes. Preliminary examination of available bathymetry from these and other segments in this larger area indicates a correlation between core complex morphology and seismicity. We suggest that detachment faulting may be more common than previously suspected in this part of the MAR. As much as 35% of the spreading axis may be experiencing detachment faulting and thus, >15% of the new seafloor accretion may be dominated by core complexes. We also suggest that the evolution of core complexes we have identified in our study area and the associated seismicity may be applicable to understanding other regions of active detachment faulting both in the oceans and on land, where the faults are more accessible but where erosion severely hinders their interpretation.

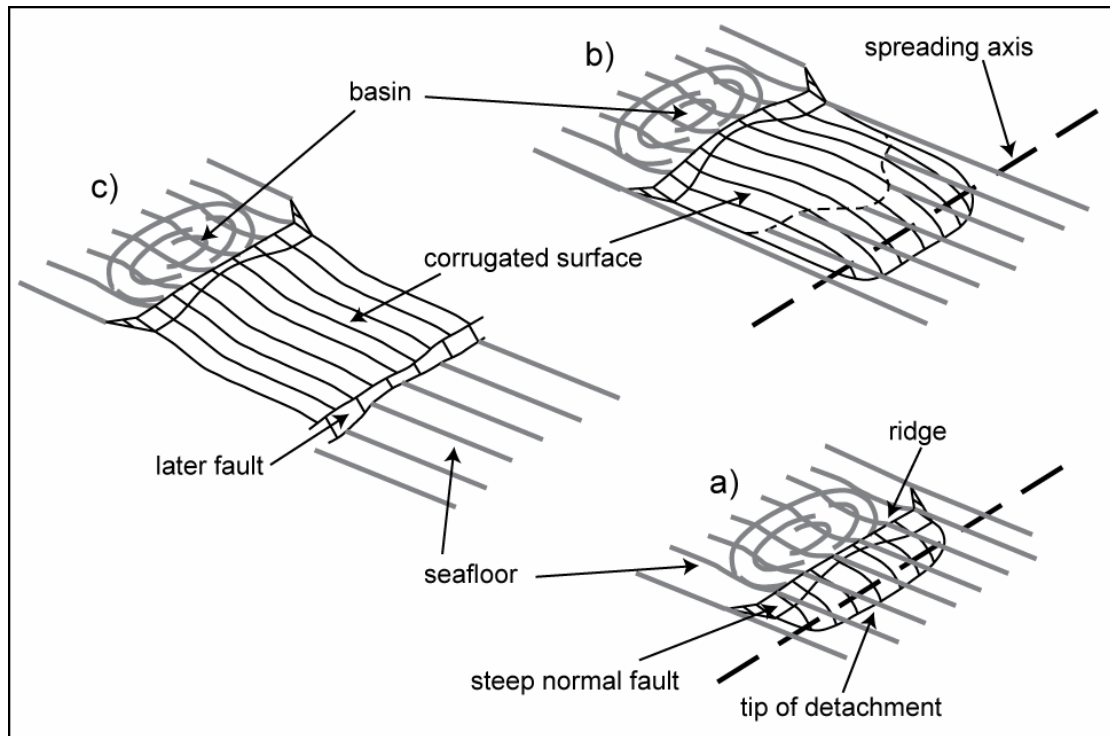


Figure 4. Schematic three-dimensional oblique view of the evolution of a core complex by detachment faulting. Gray lines: seafloor (except for the detachment surface). Black lines: surface of the detachment fault and steeper normal faults, both exposed on the seafloor and below it. a) A breakaway ridge with a basin behind it. The basin is floored by volcanic sea floor, tilted up towards the breakaway ridge. The initially steep subsurface normal fault at the breakaway has already rotated to a shallower angle. A downward-curved detachment has started to form linked to the breakaway fault. Both faults are below the seafloor. b) The detachment has emerged. Dashed line: line of emergence. The fault has warped into a dome, the ridge has become arched, and little further rotation of the initial ridge has occurred. c) The detachment fault has been cut off by a later normal fault, perhaps of the breakaway of the next detachment. The dome has flattened, and the detachment fault is inactive.

References:

- ¹ J. R. Cann, D. K. Blackman, D. K. Smith et al., *Nature* **385**, 329 (1997).
- ² B.E. Tucholke, J. Lin, and M. C. Kleinrock, *J. Geophys. Res.* **103**, 9857 (1998).
- ³ D.K. Blackman, J.R. Cann, B. Janssen et al., *J. Geophys. Res.* **103**, 21 (1998).
- ⁴ C. J. MacLeod, J. Escartín, D. Banerji et al., *Geology* **30** (10), 279 (2002).
- ⁵ J. Escartín, C. Mével, C.J. MacLeod et al., *Geochem. Geophys. Geosys.* **4**, 1067 (2003).
- ⁶ R. C. Searle, M. Cannat, K. Fujioka et al., *Geochem. Geophys. Geosyst.* **4** (9105), doi:10.1029/2003GC000519 (2003).
- ⁷ H. J. B. Dick, W. B. Thompson, and W. B. Bryan, *EOS, Transactions, American Geophysical Union* **62**, 406 (1981); J.A. Karson and H.J.B. Dick, *Mar. Geophys. Res.* **6**, 51 (1983).
- ⁸ T. Schroeder and B. E. John, *Geochem. Geophys. Geosyst.* **5** (11), 1 (2004).
- ⁹ D.M. Christie, B.P. West, D.G. Pyle et al., *Nature* **394**, 637 (1998).
- ¹⁰ K. Okino, K. Matsuda, D. Christie et al., *Geochem. Geophys. Geosyst.* **5**(12), doi:10.1029/2004GC000793 (2004).
- ¹¹ J. Escartín and M. Cannat, *Earth Planet. Sci. Letts.* **171**, 411 (1999).
- ¹² Y. Ohara, T. Yoshida, and S. Kasuga, *Mar. Geophys. Res.* **22**, 47 (2001).
- ¹³ Mathilde Cannat, Catherine Mével, Marcia Maia et al., *Geology* **23**, 49 (1995).
- ¹⁴ D. K. Blackman, J. A. Karson, D. S. Kelley et al., *Mar. Geophys. Res.* **23**, 443 (2003).
- ¹⁵ W.H.F. Smith and D.T. Sandwell, *Science* **277**, 1956 (1997).
- ¹⁶ D. K. Smith, J. Escartin, M. Cannat et al., *J. Geophys. Res.* **108**, doi: 10.1029/2002JB001964 (2003).
- ¹⁷ T. Fujiwara, J. Lin, T. Matsumoto et al., *Geochemistry, Geophysics, Geosystems* **4** (3), 1024 (2003).
- ¹⁸ S. M. Sudarikov and A. B. Roumiantsev, *Journal of Volcanology and Geothermal Research* **101**, 245 (2000).
- ¹⁹ B. E. Tucholke, K. Fujioka, T. Ishihara et al., *J. Geophys. Res.* **106** (B8), 16145 (2001).
- ²⁰ J. E. Spencer, *Geology* **27**, 327 (1999).
- ²¹ K. C. Macdonald, *Ann. Rev. Earth Planet. Sci.* **10**, 155 (1982).
- ²² D. K. Smith, M. Tolstoy, C. G. Fox et al., *Geophys. Res. Letts.* **29**, doi: 10.1029/2001GL013912 (2002).
- ²³ D. R. Bohnenstiehl, M. Tolstoy, R. P. Dziak et al., *Tectonophysics* **354**, 49 (2002); C. G. Fox, H. Matsumoto, and T-K Lau, *J. Geophys. Res.* **106**, 4183 (2001).
- ²⁴ J. Escartin, D. K. Smith, and M Cannat, *Geophys. Res. Letts.* **30** (12, 1620), doi:10.1029/2003GL017226 (2003).

Acknowledgments. We are grateful to the captain and crew of the R/V Knorr (Leg 182, 2005). We are also grateful to P.Lemmond, H. Schouten, and M. Tivey for their help in collecting the data at 13°N. We had fruitful discussions with R. Searle, H. Schouten, M. Tivey and R. Sohn. We also thank John Goff and one anonymous reviewer for their thoughtful and constructive comments on the manuscript. This work was supported by the National Science Foundation. IPGP contribution 2136.